

# DESIGN OF A DEFORMABLE VEHICLE ROOF STRUCTURE FOR ROLLOVER CRASH TESTING WITH A TEST BUCK

## Jacek Toczyski

Institute of Aeronautics and Applied Mechanics, Warsaw University of Technology  
Poland

## Jason R. Kerrigan

Center for Applied Biomechanics, University of Virginia  
United States

## Pradeep Mohan

Channabasaveshwara Institute of Technology  
India

## Jeff R. Crandall

Center for Applied Biomechanics, University of Virginia  
United States

Paper Number 13-0203

## ABSTRACT

The goal of this study was to determine the detailed design of a greenhouse structure (roof and pillars), such that when it is loaded in a static roof crush test the force-displacement response mimics that of a modern full-size crossover vehicle. This study was carried out using finite element analysis with the goal of identifying a specific design to be fabricated for use with a rollover test buck in dynamic rollover crash testing. A multi-tiered design approach was used consisting first of a simple beam element model, followed by a more complex model meshed with shell and solid elements. A truss-like structure consisting of steel tubing for the pillars, headers and roof rails, connected by steel bars (“plastic joints”) at the intersections was used for the initial design. Individual structure parameters (tubing cross-sections, wall thicknesses, material types, etc.) that did not affect the overall geometry were optimized in repeated simulations of a static roof crush test to ensure that the response of the buck roof matched the response defined by a strength-to-weight ratio of 4.0 for a 2268 kg vehicle. Additionally, different design solutions were examined, e.g. curving the B-pillar, adding a windshield or roof cross beams. The influence of the friction coefficient between the loading platen and the roof was also investigated. Model predictions were validated on component-level by comparing model behavior to three-point bending tests on the plastic joints. The resulting design, including curved B-pillars with additional stiffness elements, was then subjected to a dynamic rollover computer simulation to facilitate qualitative evaluation of the dynamic response in a rollover crash. Further modification of the design may be necessary to improve the response beyond the peak quasi-static test force, but full scale fabrication and testing will be performed first to examine actual

response at these levels before implementing additional changes.

## INTRODUCTION

Rollover related deaths are a significant portion of the overall traffic-fatalities in the United States (US). As a result of this problem, rollover crashworthiness (cf. Mohan et al. 2008) as well as injury outcome (cf. Foster et al. 2012) have long been studied by vehicle safety researchers. The National Highway Traffic Safety Administration (NHTSA) has introduced several safety standards aimed at mitigating the effect rollover crashes have on the public health, including mandating stronger roofs (Federal Motor Vehicle Safety Standard (FMVSS) No. 216), electronic stability control (FMVSS No. 126), and ejection mitigation (FMVSS No. 226) (US Department of Transportation 2012). However, currently there is no dynamic rollover test standard for crashworthiness or occupant protection, at least in part, due to the lack of demonstrated biofidelity of crash test dummies and injury metrics in rollover crash tests.

As part of a larger research effort aimed at investigating the crash dummy biofidelity in such tests, the University of Virginia Center for Applied Biomechanics is planning to compare crash test dummy response to post-mortem human surrogate (PMHS) response in multiple series of experimental investigations. To perform some of the analyses, a vehicle-like rollover test buck has been developed. It consists of two major parts: a deformable, replaceable greenhouse (roof and pillars) and a rigid base. The buck has been designed to mimic the geometric and inertial properties of the average of twelve full-size crossover vehicles from the current fleet. The buck will be used in the biofidelity tests for a variety of reasons. Primarily, real vehicle interiors have very complex geometries and complex

material properties. Since such complex structures could feasibly have an effect on occupant kinematics, exact or very similar structures would be necessary to make comparisons between occupant surrogates. Thus, evaluations of dummies modified after initial tests will need to be made with the same structures or a detailed computational model of them. Since such evaluations may be made years after original tests, a simplified buck is used to ensure that replicate structures can be fabricated or simulated easily. Secondly, 3-d optical motion capture systems that have been used to characterize occupant surrogate motion in simulated crash tests (cf. Lessley et al. 2010) require line of sight between off-board cameras and on-board occupant retroreflective markers. Using such a system will provide detailed 3-d kinematics data that can be used to make intricate comparisons between crash test dummies and PMHS. Lastly, unlike real vehicles, a rollover test buck provides a platform for vehicle parameter sensitivity analysis where individual parameters (mass, moment of inertia, seating location, restraint geometry, roof geometry, roof strength, etc.) can be adjusted.

While design of a base structure (that matches the goal geometry and inertial properties) is a relatively easy goal, design of a roof structure with a crushing stiffness that is comparable to real vehicles is more challenging. The use of a replaceable roof buck to evaluate variations in vehicle and occupant parameters has been previously investigated (Jordan et al. 2005). That study concluded that a test buck can be used in rollover crash test studies to examine some characteristics of occupant and vehicle response.

The goal of this study was to determine the detailed design of a greenhouse with large tumblehome angles (ca. 80°), such that when it is loaded in a static roof crush test (similar to the FMVSS No. 216 test) the force-displacement response mimics that of a vehicle with a strength-to-weight ratio (SWR) of 3.9-5.3 (depending on the total buck mass). The study was carried out using finite element analysis to facilitate computationally and monetarily inexpensive evaluations of iterative changes to the design. In studies subsequent to the current one, the resulting buck roof design will be fabricated and tested in static roof crush to evaluate the accuracy of the computational predictions.

## BUCK DESIGN

A parametric rollover test buck was developed for use with the Dynamic Rollover Test System (DRoTS) (Kerrigan et al. 2011a) to investigate dummy biofidelity in rollover crash impacts. It was designed to have a rigid base, consisting of all the components below the simulated vehicle belt-line,

and a deformable (and thus replaceable) roof structure, consisting of all the components above the belt line (roof, pillars, headers, cross beams). The base structure (Figure 1) consists of A-, B-, C- and D-pillars, front and rear pillar connections, and removable “doors.”

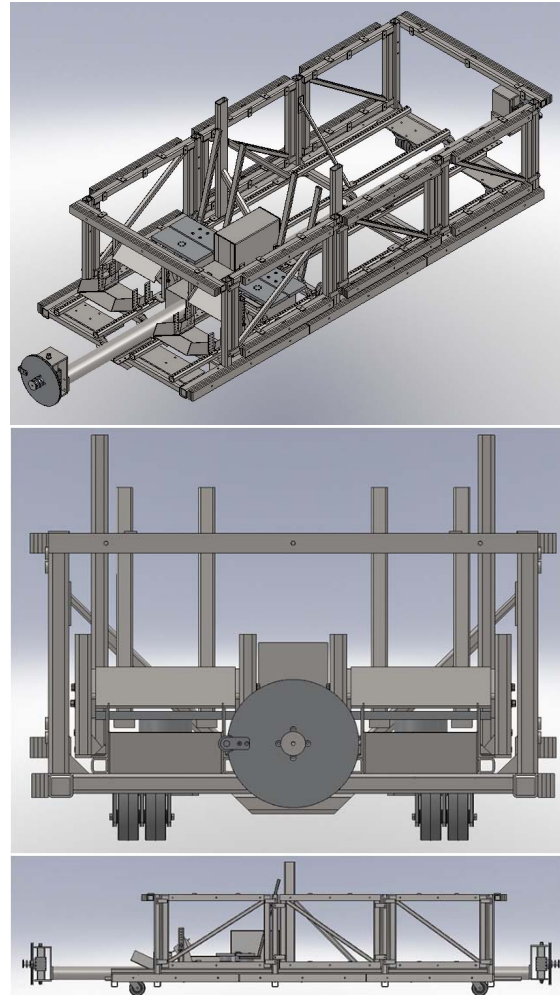


Figure 1. Base structure of rollover test buck: isometric (top), front (middle) and side view (bottom).

The buck was designed to mimic the geometric and inertial properties of twelve late-model full-sized crossover vehicles or mid-sized sport utility vehicles (SUV) from the US fleet, including BMW X5, Ford Explorer, Jeep Grand Cherokee, Kia Sorrento, Volvo XC90 and Volkswagen Touareg. Exterior geometric properties of the vehicles were determined from New Car Assessment Program (NCAP) test reports and they were averaged to specify general dimensions for the buck base (Foltz et al. 2011). The validity of exterior dimensions extracted from the reports was verified by manual measurements made on three of the vehicles. Inertial properties – mass, center of gravity (CG) location, and roll moment of inertia – were either

established or estimated from the literature (Bixel et al. 2010, Heydinger et al. 1999) and consumer marketing materials. Interior geometries of the vehicles, including measurements of the head, leg, shoulder, and hip room in the first and second row seats were determined (also using consumer marketing materials) to vary only minimally across the entire set of considered cars. Maximum coefficient of variation for any measurement was 6%. As a result, detailed measurements were made manually on three of the twelve vehicles, to determine specific interior geometry goals for the buck, including seat to roof / pillar / console / instrument panel distances, overall interior width / height / length, and door opening geometry. Using these geometric definitions, a center console, simple rigid seats, knee bolsters, toe pans and belt D-ring mounting posts were designed to generally match the interior geometry of the vehicles. The occupant seating and restraint hardware can be adjusted in all three dimensions. Most of the buck mass is contained near the CG in a 127 mm diameter solid steel bar. The location of this bar relative to the occupant seating area can be adjusted vertically to simulate variations in the vehicle CG. Additionally, ballast can be added at various locations to adjust the overall mass (1690-2326 kg) and moment of inertia (580-850 kg m<sup>2</sup>) to achieve the extremes of the distribution from the twelve fleet vehicles.

Examination of the roof geometry data for the considered vehicles showed that the greatest variation was in the shape of the roof. Particularly, the tumblehome angles of the roof structure, and the lateral curvature of the roof seemed to vary widely, with some vehicles having a lower tumblehome angles and curved roofs, and some having fairly flat roofs and steep tumblehome. As a result, two different roof/pillar geometries were determined for the buck to represent variations in the fleet. These two roof geometries varied in a shape parameter, which was defined as the difference between the vehicle CG to roof rail distance (the maximum radius) and the vehicle CG to roof center distance. This parameter estimated the “roundness” of the vehicle with larger values describing a less round shape and smaller values describing a more round shape. The parameter varied across the twelve fleet vehicles from 52 mm to 153 mm (mean: 99 mm, standard deviation: 32 mm). Roof 1 was designed to have a shape parameter of 69 mm (a rounder roof), and Roof 2 was designed to have a shape parameter of 135 mm (a more “boxy” roof). For the purpose of this study, only Roof 2 was considered in the computational analyses, as it will be fabricated and tested first. To determine roof strength or stiffness goal for the buck roof structure, data from Insurance Institute for Highway Safety (IIHS) roof crush testing was

used. Much like the FMVSS No. 216, “Roof crush resistance” test, the IIHS test involves quasi-static loading of the vehicle roof, at a 25 degree roll and 5 degree pitch angle, with a rigid platen. The platen is driven into the vehicle for a distance of 254 mm, and the peak reaction force on the platen generated in the first 127 mm of deformation is normalized by the vehicle weight to determine the strength-to-weight ratio (IIHS 2012). It was assumed that the majority of new vehicles would have strength-to-weight ratios of 4.0 or above, and thus the buck was designed to have a roof with a SWR of 4.0 at its maximum mass (approximately 2268 kg). Data from the IIHS tests were analyzed to determine the general shape of the force-deformation response of the vehicles (Figure 2).

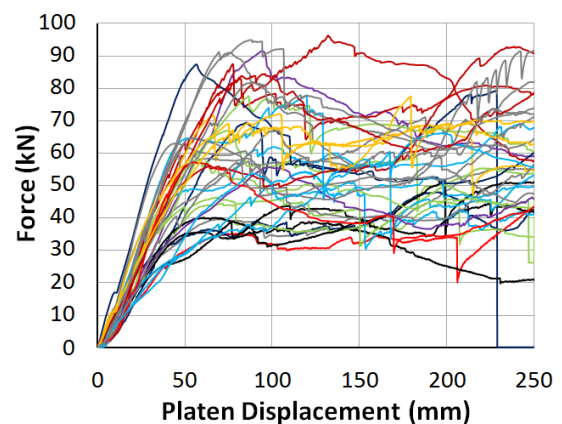


Figure 2. Roof crush force vs. platen displacement for 37 vehicle tests (IIHS 2012).

Based on this data, a goal force-displacement response for the buck roof under quasi-static platen loading at 25 degrees roll and 5 degrees pitch was identified (Figure 3). The goal response should increase approximately linearly from 0 N to the peak force (88.9 kN) over the first 75 mm of deformation, and then remain at an approximately constant force beyond that deformation.

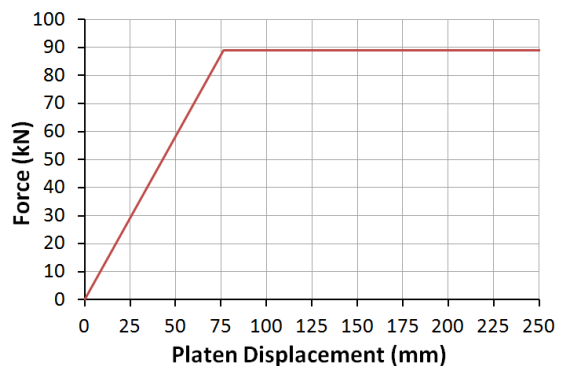


Figure 3. Desired force-deformation response for the roof structure.

## METHODS

### Initial design

Once the specific geometry of the roof (Roof 2) was determined, a baseline design of the greenhouse structure was created. The design utilized components that could be readily purchased or easily machined. Round tubing was used for the pillars, the roof rails, the windshield header, and connections between the tops of the B-, C- and D-pillars (Figure 4). Additional hat-section beams were used to connect right and left roof rails between the A- and B-, and the B- and C-pillars.

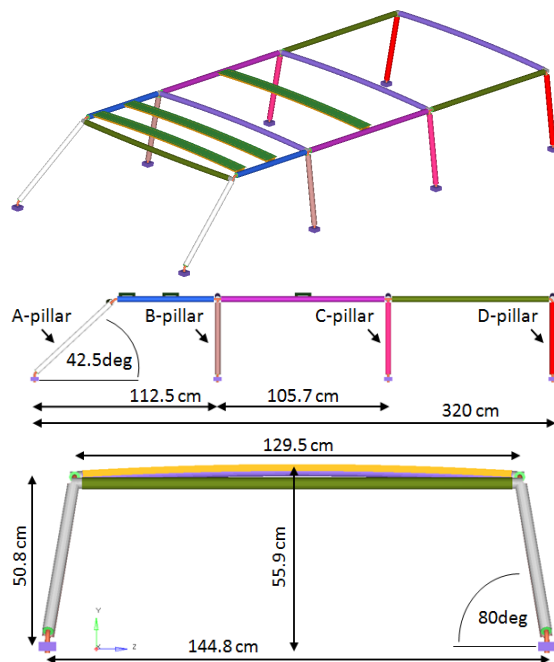


Figure 4. FE model of the initial design of the roof structure.

Plastic joints, consisting of a round bar set into the tube ends (Figures 5 & 6), were used to join tubing at the interfaces between the pillars, roof rails, headers, and additionally at connections between the pillars and the rigid buck base. The joints are made of 1018 low carbon steel, the tubing is manufactured of 1010 or 1020 steel.

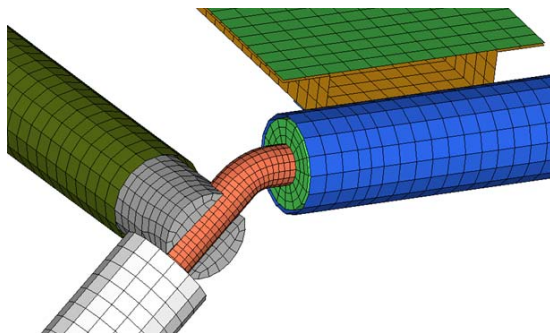


Figure 5. FE Model detail of the A-pillar, windshield header, roof rail intersection.

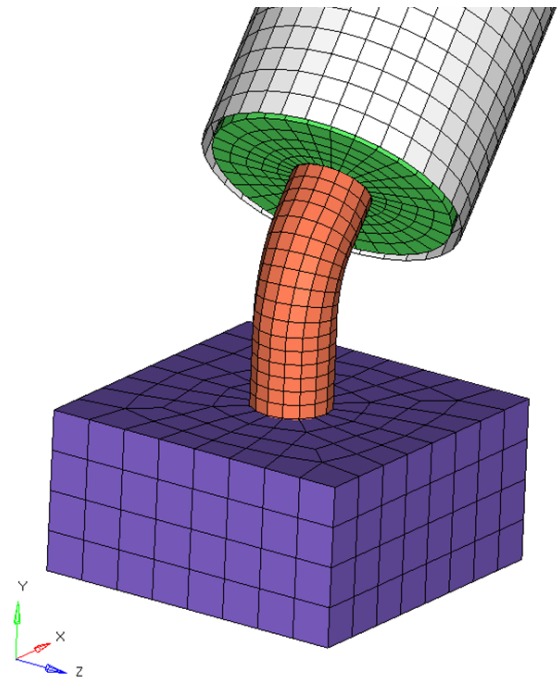


Figure 6. FE Model detail of the A-pillar/beltline interface.

### Computational investigation

Each of the plastic joints, tubing and header sections were sized by performing a detailed computational investigation using a commercial implicit finite element (FE) code (Abaqus 6.11-3). A multi-tiered design approach was used consisting first of a simple beam element model (Figure 7), followed by a more complex model meshed with shell (tubes, hat section beams) and solid (plastic joints and inserts) elements. Interfaces between components which are going to be welded in the fabricated structure were modeled using shared nodes (simplified model) or a tied contact (detailed model).

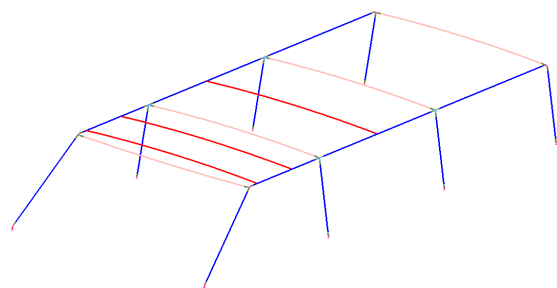


Figure 7. Beam element model of the greenhouse.

Elastic-plastic material models were used to describe the behavior of different steels used for different parts of the roof. The nonlinear stress-strain relationship beyond the yield point was defined as tabular data in the numerical models. The properties were taken from the literature

(Sabih et al. 2012, Padmanabhan et al. 2008, Schaeffer et al. 2007) and validated through three-point bending tests (Figure 8).

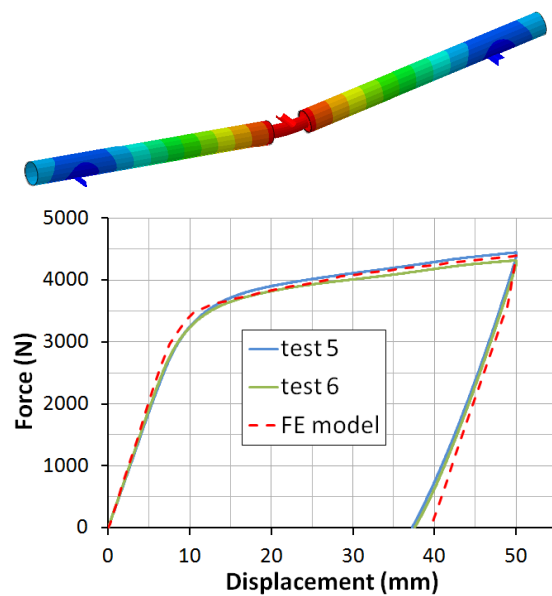


Figure 8. 3-point bending test of a plastic joint buck component: experiment (top), numerical simulation (fringe: resultant displacement; middle) and force vs. displacement comparison (bottom).

Using the FE models, sensitivity studies were carried out to evaluate component sizes, beam curvature and alignment, the number of structural connections and cross beams and the effect of a windshield. For each component of the roof structure cross-sectional shape, dimensions and material properties were assigned. Each parameter was adjusted separately in an iterative fashion. Only the geometry of the individual components was adjusted, and the overall geometry of the greenhouse remained the same. Also, the addition of other structural components was evaluated to determine effects on the overall mechanical behavior.

Most of the simulations were performed with the use of the beam element model (“the simplified model”). The use of the simplified model allowed for keeping the wall clock time of a single

simulation on a reasonable level (between 15 and 30 minutes). When the force-deformation response of the simplified model was satisfactory, it was assessed using the detailed model. Comparisons between the simplified and the detailed model were made with the initial and final design to verify the validity of the simplified model.

Lastly, the final design was evaluated in a dynamic rollover crash computer simulation. To do this, the bases of all the pillars were tied rigidly to a single mass element located at the approximate CG of the entire buck (with the roof added). The mass and inertial properties were chosen from one of the twelve full-sized crossover vehicles used to design the buck ( $m = 2002 \text{ kg}$ ,  $I_{xx} = 838.5 \text{ kg m}^2$ ,  $I_{yy} = 3399 \text{ kg m}^2$ ,  $I_{zz} = 3630 \text{ kg m}^2$ ). The buck was oriented and provided initial velocities (at initial contact) using touchdown parameters (Table 1) extracted from an unpublished deceleration sled test (similar to Kerrigan et al. 2011b) performed on one of the twelve vehicles. Local axes are defined using the Society of Automotive Engineers (SAE) convention for vehicles and global axes are defined to be aligned with the vehicle coordinate system prior to the vehicle’s lateral trip.

Table 1. Touchdown parameters for the dynamic test.

Parameter	Value
Roll Angle (deg)	-181
Pitch Angle (deg)	2.5
Yaw Angle (deg)	7.7
Local X-Angular Velocity (deg/s)	-228
Local Y-Angular Velocity (deg/s)	-8.9
Local Z-Angular Velocity (deg/s)	-23.4
Global X-Velocity (m/s)	0.2
Global Y-Velocity (m/s)	-3.5
Global Z-Velocity (m/s)	2.7

To perform an explicit dynamic rollover simulation the detailed model was converted from ABAQUS 6.11-3 to LS-Dyna V971 R4.2.1.

## RESULTS

### Evaluation of initial design

In the first loop of numerical simulations the force-displacement response of the greenhouse described in the “Initial design” section was evaluated. Comparison of the detailed and simplified models indicated that the simplified model could provide a relatively accurate response of the full model (Figure 9). While the models showed similar mechanical behavior, the value of a peak force was higher (about 15%) in the beam element model. The “beam” response is also smoother; connections between components were modeled in a very simple way that prevented local effects (e.g.

buckling) from appearing in the global force-deformation response.

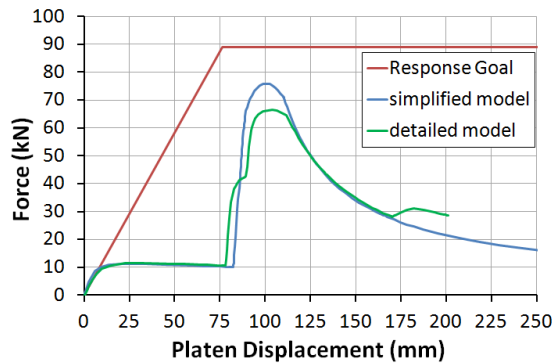


Figure 9. Force-displacement response of initial design.

It was clear that the greenhouse was much too soft over first 80 mm of deformation as well as after 120 mm. Additionally, it was noticed that the response showed a discontinuity around 80 mm of the roof displacement. It was determined that this discontinuity was caused by the platen contacting and loading the B-pillar. The pillar started being compressed and the axial force acting on it became the dominant force acting on the entire structure. It resulted in a very large increase of the crushing force – from 10 kN up to 65-75 kN.

The final deformation of the greenhouse at the end of the numerical analyses showed a “matchbox” effect where the far side pillars were pushed more vertically, and then beyond, whereas the near side pillars were bent inward (Figure 10). No visible plastic deformations in most of the tubes and top cross beams were seen, and only the plastic joints incurred permanent deformations.

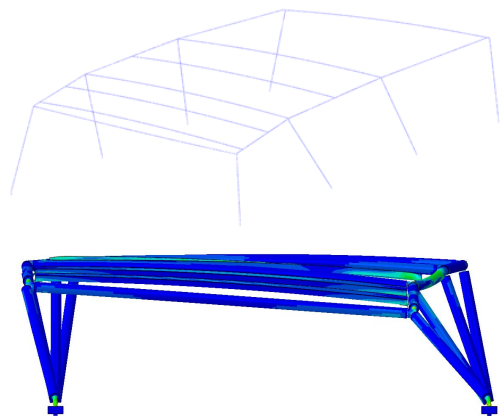


Figure 10. Final deformation of the greenhouse (initial design): isometric view, simplified model (top); front view, detailed model (bottom).

#### Parametric studies – friction/joint diameter

These initial simulations showed that there was significant sliding between the platen and the tube

structure. To evaluate the influence of the friction between the platen and the roof, a sensitivity study was performed for different values of the friction coefficient. The force-displacement response was heavily dependent on the friction values (Figure 11). The value of a peak force for a friction coefficient of 0.9 was almost eight times higher than for a coefficient of 0.35.

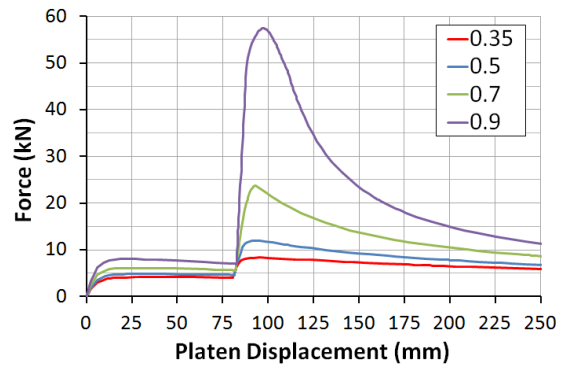


Figure 11. Force-displacement response for different friction coefficients.

Using a friction coefficient of 0.9 the influence of the plastic joint diameter was evaluated in another sensitivity study. As a first step, simulations were performed where every plastic joint in the structure had the same diameter, and diameters readily available for purchase were evaluated (Figure 12). The simulation results showed that there was a slight increase of the force value at the very beginning of the crushing process for the various diameters. After that there was a plateau until the platen came into contact with the B-pillar (~82 mm of platen displacement). The force reached its maximum at 90-100 mm of deformation and then began decreasing nonlinearly. The peak force increased by almost a factor of 2 from a 50% increase in the bar diameter. For the thicker plastic joints numerical instabilities occurred and the analyses terminated due to a not converged solution.

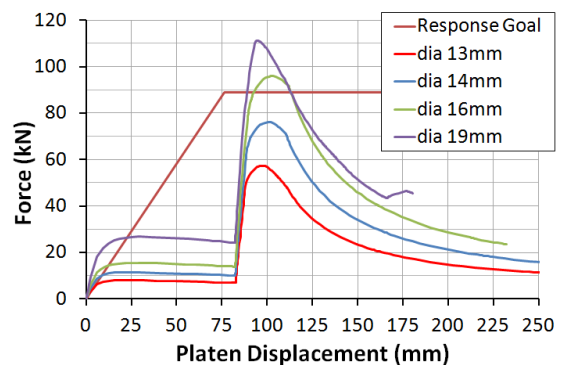


Figure 12. Force-displacement response for different plastic joint diameters.

## Improvements in the roof structure

To improve the response of the greenhouse over first 80 mm of platen displacement several different design solutions were proposed and analyzed: curving the B-pillar, adding a windshield, adding cross beams in the roof area or window area between the A- and B-pillars. The windshield was modeled as two steel bars connected in a “cross” orientation between the A-pillar tops and the opposite side A-pillar bases. Cross beams (bars) in the window areas connected the tops of the A-pillars to the bases of the B-pillars. Roof cross beams (bars) were used instead of the hat section beams and they connected the tops of the A-pillars to the tops of the opposite side B-pillars (Figure 13). For each configuration, simulations using the simplified model were performed.

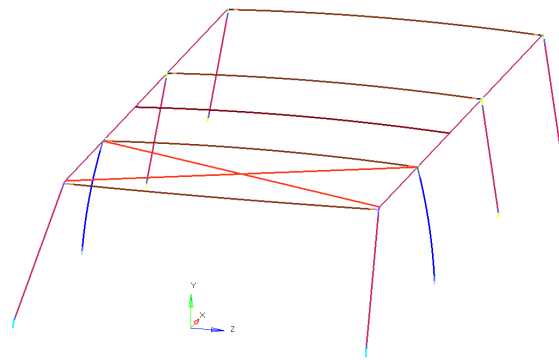


Figure 13. Greenhouse structure with cross beams in the roof area.

Introducing bending to the B-pillar decreased the critical force needed to get the pillar to buckle. Curving it with a 2.26 m radius in the Y-Z plane (SAE vehicle coordinate system reference) of the roof structure reduced the value of a peak force by approximately 45% (Figure 14) and changed the character of the response significantly, especially in the rate of force reduction after the peak force occurred.

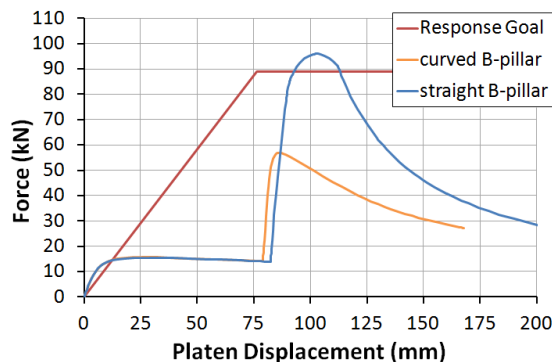


Figure 14. Force-displacement response for straight and curved B-pillar.

The addition of the roof cross beams, the window cross beams, or the windshield cross did not change the global response or the peak force substantially (Figure 15). The addition of the roof cross beams slightly shifted the displacement where the discontinuity occurred. The window cross beams and the simulated windshield increased the initial stiffness and then shifted the discontinuity to a lower (windshield) or higher (window cross beams) deformation level.

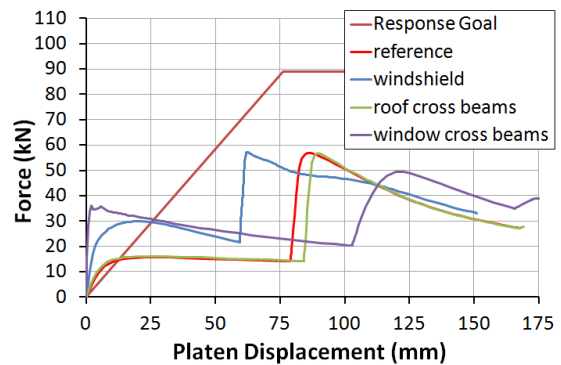


Figure 15. Force-displacement response for analyzed solutions. The reference simulation included the curved B-pillar (Figure 14).

## Final design of the Roof 2 structure

Based on the performed simulations a new design of the greenhouse was proposed. In the B-pillar area, two more components were added (Figure 16). The first element was a curved steel tube (outer diameter: 25 mm). The second was a curved steel bar with a 16 mm diameter. Both of the members originated from the base of the B-pillar and rose to the roof rail in the front-row window area. These components were added to increase the stiffness of the overall structure prior to engaging the B-pillar.

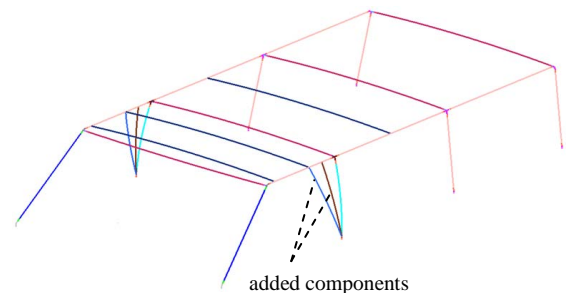


Figure 16. Greenhouse with added components in the B-pillar area.

The force-displacement response of the new design can be divided into several phases (Figure 17). During the first phase (0-30 mm) the platen pushed the A-pillar and the roof rail inwards. After 30 mm of roof displacement the platen hit the first added element (curved steel tube), which caused a large

increase in global stiffness. After about 50 mm of displacement, the next component (steel bar) was engaged, which increased the stiffness again. Similarly, around 70 mm the B-pillar was loaded, which again increased the stiffness. The force reached its maximum value (90 kN) and started decreasing nonlinearly until 160 mm of deformation when the rear edge of the platen contacted the BC-roof rail, which resulted in a small increase of the force. After 235 mm of the roof displacement a significant change in the response was observed when the platen hit the middle section of deformed (bent) added pieces.

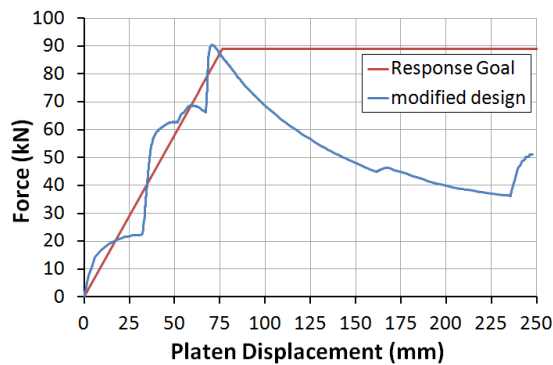


Figure 17. Force-displacement response for the modified design.

The resulting response mimicked that of a vehicle – with a strength-to-weight ratio of 4 – very well over first 75 mm of platen movement. While the response of the roof beyond 75 mm needs to be improved to achieve a constant force goal, the predicted response is not uncommon relative to real vehicles (Figure 2).

To evaluate the response of the considered design the detailed model of it was used. The added components were connected to the AB-rail and the B-pillar through steel C-channels (Figure 18). Detailed connections at each of the joints were implemented to model the fabricated structure as closely as possible.

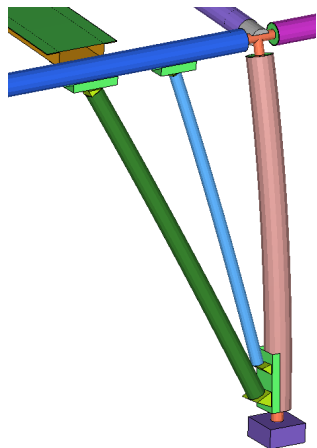


Figure 18. B-pillar area with added components.

The detailed model showed a slightly different response than the simplified model (Figure 19), but overall model response showed agreement in stiffness and peak force. The detailed model showed convergence problems beyond 217 mm of deformation. Structural deformations showed that once the B-pillar and added components began bending, far-side pillar deformations ceased and matchboxing reduced (Figure 20).

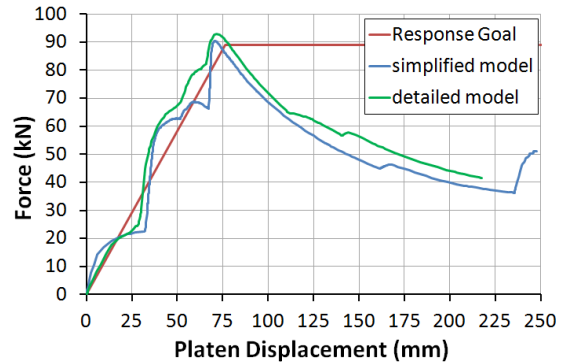


Figure 19. Force-displacement response for the simplified and the detailed model of the modified greenhouse design.

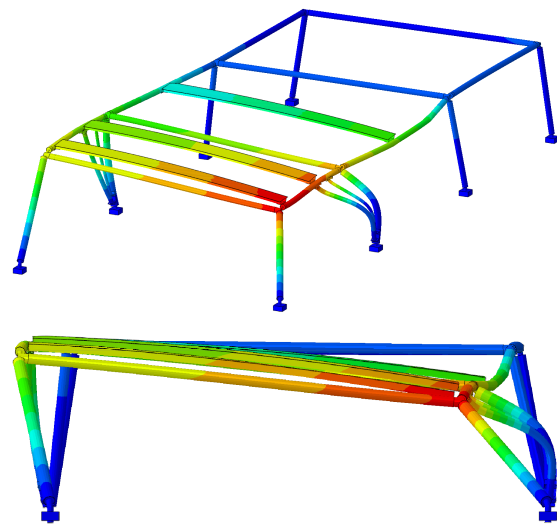


Figure 20. Greenhouse deformation at platen displacement of 217 mm: isometric view (top); front view (bottom).

### Dynamic rollover crash simulation

The resulting design was subjected to a dynamic rollover computer simulation to facilitate qualitative evaluation of the dynamic response in a rollover crash (Figure 21). For the simulation, the friction coefficient between the ground and the roof structure was established as 0.4.

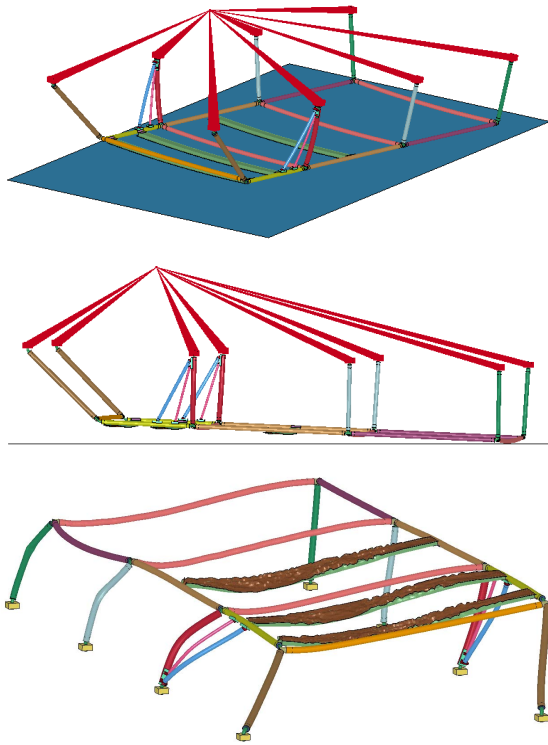


Figure 21. The vehicle at initial contact with the ground: isometric view (top); side view (middle), and final deformation of the roof structure (bottom).

The data (Figure 22) and visualization output showed that the buck, which was initially pitched with the rear end down and the front end up, pitched forward during the simulation to load the trailing-side A-pillar. This occurred since the center of gravity (Figure 21) was located forward of the initial touchdown location, which resulted in a pitching moment generated by the initial rear end contact. Similarly, despite to the initially negative yaw velocity, the buck increased its (positive) yaw angle throughout the simulation due to the initially-high yaw moment that occurred. This yaw moment resulted from the location of the center of gravity relative to the initial contact location and the translational (over the ground) velocity. Lastly the exchange of energy between rotation and translational energy typical in rollover crashes (cf. Funk et al. 2012) was evident in this case also (Figure 23). The roof's contact point initially had a tangential velocity greater than that of the buck CG's translational velocity, and thus, energy was initially transferred from rotation to translation which resulted in a decrease of the angular rate and an increase of the translational velocity. However, when the translational velocity became equal to the tangential velocity, both terms began to decrease.

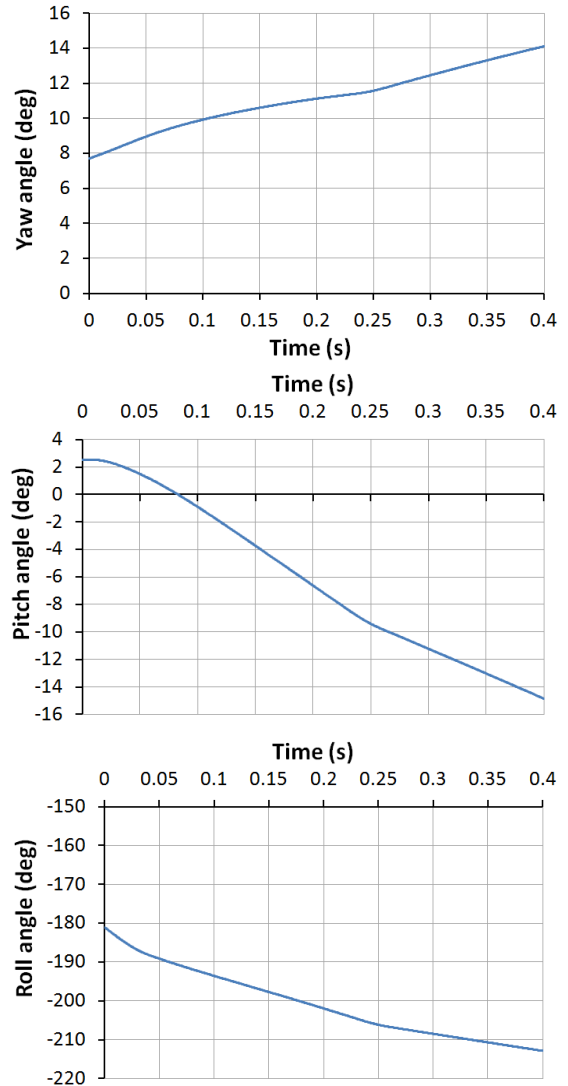


Figure 22. Time histories of the Yaw (top), Pitch (middle) and Roll (bottom) angles.

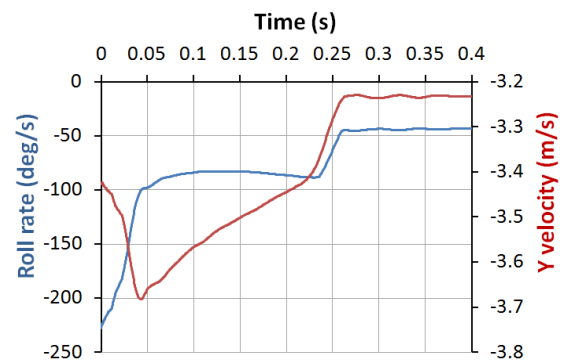


Figure 23. Roll velocity and lateral (Y-axis) translational velocity time histories from the dynamic simulation.

The peak vertical force was 110 kN, which occurred at approximately -187 degrees of roll angle (Figure 24). Previous testing has shown that peak forces between 110 kN and 120 kN between

the vehicle and the ground in a single roof-to-ground rollover crash test are realistic for an SUV (Pontiac Torrent) with a relatively high strength-to-weight ratio (Kerrigan et al. 2013). Ideally, dynamic response data would be compared directly to actual test data for a similarly shaped vehicle with similar inertial properties and roof strength; however, such data could not be identified from the literature.

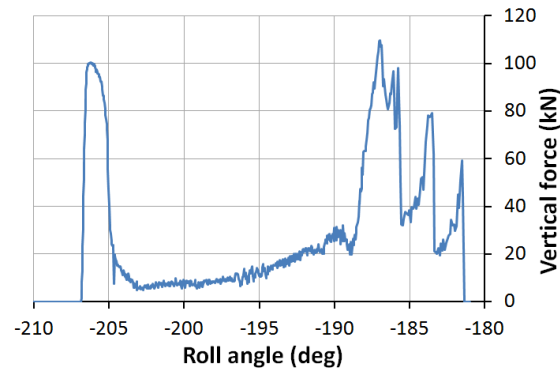


Figure 24. Force-roll angle time history for the buck.

## DISCUSSION

Since the buck was designed to simulate the response of real vehicles in a dynamic rollover crash test, using dynamic response targets for the model iterations would have been ideal. However, standardized dynamic test data for a variety of vehicles is not available. As a result, quasi-static roof crush data were used to determine a generally representative response of vehicles in the fleet. While many vehicles show an initially steep increase to the maximum force, followed by a decrease in force over larger deformations in a FMVSS No. 216-like test, the modeling target was designed for a constant force after the peak to generally represent the fleet surveyed (Figure 2). Based on the performed FE simulations the baseline design was modified and converted into a greenhouse that has a force-deformation response that generally matches a real vehicle with a high strength to weight ratio. This was accomplished by modeling off-the-shelf parts and in a way that will make it easily fabricated. The model parameters could now be scaled to create a weaker/stronger model, which still has the same overall geometry. These models could be used to evaluate the effect of roof strength in a dynamic test without changing the critical-to-the-design external dimensions of the structure. It is also worth mentioning that the real value of a friction coefficient between the platen and the roof structure was not determined, but a substantial sensitivity was shown. As a result, until static roof crush testing can be completed, there is no way to

determine how large the difference between the simulation prediction and the test result will be.

## CONCLUSION

The goal of this study was to determine a detailed design for a roof structure to be used to perform rollover crash tests with a rollover test buck. Variations in an initial design of the greenhouse and computational analyses yielded a model that has a loading response that is representative of a modern full-size crossover vehicle. Further modification of the design may be necessary to improve the response beyond the peak quasi-static test force, but full scale fabrication and testing will be performed first to examine the actual response at these levels before implementing additional changes. When the final design is fabricated and the model predictions are validated in a real test meeting FMVSS No. 216, the test buck with the greenhouse attached will be used to evaluate dummy biofidelity in future matched PMHS and dummy rollover crash tests. Computational modeling of the more “round” roof structure (with smaller tumblehome angles) is also considered as one of the next steps in this research.

## ACKNOWLEDGMENTS

This study was supported in part by the National Highway Traffic Safety Administration (NHTSA) under Cooperative Agreement No. DTNH22-09-H-00247. This study was also supported in part by the European Union in the framework of European Social Fund through the “Didactic Development Program of the Faculty of Power and Aeronautical Engineering of the Warsaw University of Technology.” Views or opinions expressed or implied are those of the authors and are not necessarily representative of the views or opinions of the NHTSA or the Warsaw University of Technology.

## REFERENCES

- [1] Bixel, R.A., Heydinger, G.J. and D.A. Guenther. 2010. “Measured vehicle center-of-gravity locations – including NHTSA’s data through 2008 NCAP.” Society of Automotive Engineers (SAE). Paper Number 2010-01-0086. Warrendale, PA
- [2] Foltz, P., Kim, T., Kerrigan, J.R. and J.R. Crandall. 2011. “Vehicle greenhouse shape analysis for design of a parametric test buck for dynamic rollover testing.” In Proceedings of the 22nd International Technical Conference on the Enhanced Safety of Vehicles (ESV) (Washington, D.C., June 13-16)

- [3] Foster, J.B., Kerrigan, J.R., Nightingale, R.W., Funk, J.R., Cormier, J.M., Bose, D., Sochor, M.R., Ridella, S.A., Ash, J.H. and J.R. Crandall. 2012. "Analysis of cervical spine injuries and mechanisms for CIREN rollover crashes." In Proceedings of the 2012 IRCOBI Conference (Dublin, Ireland, Sep 12-14)
- [4] Funk, J., Wirth, J., Bonugli, E., Watson, R. and A. Asay. 2012. "An integrated model of rolling and sliding in rollover crashes." SAE Technical Paper 2012-01-0605. doi: 10.4271/2012-01-0605
- [5] Heydinger, G.J., Bixel, R.A., Garrott, W.R., Pyne, M., Howe, J.G. and D.A. Guenther. 1999. "Measured vehicle inertial parameters – NHTSA's data through November 1998." Society of Automotive Engineers (SAE). Paper Number 1999-01-1336. Warrendale, PA
- [6] Insurance Institute for Highway Safety (IIHS). 2012. Crashworthiness evaluation roof strength test protocol (version II). December 2012. [http://www.iihs.org/ratings/protocols/pdf/test\\_protocol\\_roof.pdf](http://www.iihs.org/ratings/protocols/pdf/test_protocol_roof.pdf)
- [7] Jordan, A. and J. Bish. 2005. "Repeatability testing of a dynamic rollover test fixture." In Proceedings of the 19th International Technical Conference on the Enhanced Safety of Vehicles (ESV) (Washington, D.C., June 6-9)
- [8] Kerrigan, J.R., Dennis, N.J., Parent, D.P., Pursezov, S., Ash, J.H., Crandall, J.R. and D. Stein. 2011b. "Test system, vehicle and occupant response repeatability evaluation in rollover crash tests: the deceleration rollover sled test." International Journal of Crashworthiness, 16(6): 583-605
- [9] Kerrigan, J.R., Jordan, A., Parent, D., Zhang, Q., Funk, J., Dennis, N.J., Overby, B., Bolton, J. and J.R. Crandall. 2011a. "Design of a dynamic rollover test system." Society of Automotive Engineers (SAE). Paper Number 2011-01-1116. Warrendale, PA
- [10] Kerrigan, J.R., Seppi, J., Lockerby, J., Foltz, P., Overby, B., Bolton, J., Kim, T., Dennis, N.J. and J. Crandall. 2013. "Test methodology and initial results from a Dynamic Rollover Test System." Society of Automotive Engineers (SAE). Paper Number 2013-01-0468. Warrendale, PA.
- [11] Lessley, D., Shaw, G., Parent, D., Arregui-Dalmases, C., Kindig, M., Riley, P., Pursezov, S., Sochor, M., Gochenour, T., Bolton, J., Subit, D., Crandall, J.R., Takayama, S., Ono, K., Kamiji, K. and T. Yasuki. 2010). "Whole-body response to pure lateral impact." Paper Number 2010-22-0014. Stapp Car Crash Journal 54: 289-336
- [12] Mohan, P., Cing-Dao, K. and J. Riley. 2008. "Evaluation of roof strength under multiple loading conditions." In Proceedings of the 2008 International Journal of Crashworthiness Conference (Kyoto, Japan, July 22-25)
- [13] Padmanabhan, R., Oliveira, M.C. and L.F. Menezes. 2008. "Deep drawing of aluminium-steel tailor-welded blanks." Materials and Design 29: 154-160
- [14] Sabih, A. and J.A. Nemes. 2012. "Experimental and finite element simulation study of the adiabatic shear band phenomenon in cold heading process." Journal of Materials Processing Technology 212: 1089-1105
- [15] Schaeffer, L. and A.M.G. Brito. 2007. "FEM numerical simulation and experimental investigation on end-forming of thin-walled tubes using a die." Steel Research International 78, No. 10-11: 789-803
- [16] U.S. Department of Transportation, National Highway Traffic Safety Administration. 2012. Federal Motor Vehicle Safety Standards and Regulations. DOT HS 808 878. <http://www.nhtsa.gov/cars/rules/import/fmvss/index.html>